Science Press

ARTICLE

Effect of Si on High Temperature Oxidation Characteristics of Laser Cladding 625 Alloy

Zhang Jian,   Liu Zongde,   Ma Herong,   Li Yue,   Li Jiaxuan

Key Laboratory of Power Station Energy Transfer Conversion and System, Ministry of Education, North China Electric Power University, Beijing 102206, China

Abstract: The high temperature oxidation behavior of 625 alloy cladding layer with different Si contents was studied by cyclic oxidation method after 144 h oxidation at 700, 800 and 900 °C. The oxide phase was analyzed by XRD. The surface and cross section morphology, elemental composition and oxide film thickness were studied by SEM/EDS. The results show that the oxidation kinetics of the samples at different temperatures keep a parabolic law, and the oxidation mass gain increases gradually with the increase of temperature. The oxidation film of 0wt% Si 625 alloy cladding sample peels off in a large area at 900 °C, while the oxidation film of 3wt% Si alloy cladding sample remains intact. With the increase of Si content at 700 °C, the oxidation particles on the surface of the oxide film decrease in size and become denser, which promotes the formation of Cr_2O_3. At 700 °C, a large area of internal oxidation appears in 0wt% Si sample, there are two strip oxides containing Ni, Cr and Mo in the substrate of 1wt% Si sample, while the inner oxidation of 3wt% Si samples is prevented due to the formation of Si-rich inner oxidation layer. The combined effect of the outer layer of Cr_2O_3 oxide film and the inner layer of SiO_2 not only prevents the infiltration of O anions but also inhibits the diffusion of Fe and other metal ions, thus improving the oxidation resistance of the alloy cladding.

Key words: laser cladding; 625 alloy; oxidation kinetics; oxidation film; diffusion

---

In recent years, the energy structure of various countries is still dominated by coal mines. The influence of greenhouse effect and the proposal of "emission peak and carbon neutrality" require us to improve thermal power generation technology. The most suitable method is to use ultra-supercritical thermal power generation technology. Long-term work under high parameters will lead to oxidation and corrosion of equipment pipes, which will seriously reduce the service life of the unit. Therefore, it is the key to seek alloys with good high temperature resistance and oxidation resistance.

As a kind of superalloy, Ni-base alloy is widely used in various fields[1-4]. Corrosion resistant elements (such as Cu, Cr, Mo, Al) are usually added to alloys to improve their properties. However, adding elements with oxidation resistance will increase the production cost and reduce the mechanical properties of the material[5,6]. Therefore, non-metallic elements such as Si can be selected to improve the

properties of the alloy. Much attention has been paid to Si due to its availability, low cost, and antioxidant potential[4-7]. Although some studies have mentioned that the addition of Si can increase the oxidation rate[8,9], most of the literature shows that the addition of Si can enhance the oxidation resistance. Jing et al[10] studied the effect of Si addition on the oxidation resistance of Zr-Si-N nanocomposite films, and the results showed that the addition of Si can inhibit the inward diffusion of oxygen and the cracking of oxide skin, and significantly improve the oxidation resistance of the films. Yun et al[11] studied the effect of Si on the cyclic oxidation of Ni-Cr-W-Mo alloys, and the results show that Si can inhibit the generation of transient oxides, thus reducing the oxidation rate.

625 alloy is widely used as a nickel-based deformed superalloy[3,12] and has become a candidate material for key equipment of new ultra-supercritical power generation units. However, in practical engineering applications, the direct application of 625 alloy to the generator set will lead to

excessive cost, up to tens of thousands of dollars per ton. Therefore, this situation can be improved by laser cladding technology[12-14], which can not only effectively protect power generation equipment, but also save costs. In general, 500~1000 μm laser cladding layer is closely combined with the matrix, with low dilution rate and no porosity crack, which can make the surface of boiler, steam turbine and other equipment obtain good corrosion resistance and oxidation resistance. Scendo et al[15] studied the electrical corrosivity of laser cladding layers generated from 625 alloy powder and metal wire under chloride acid condition, and the results showed that the laser cladding layers produced from powder show good corrosion resistance. Liu et al[5] studied the effect of Si on the corrosion resistance of Ni-Cr-Mo-W-xSi laser cladding layer in H_2S atmosphere by preparing Ni-Cr-Mo-W-xSi laser cladding layer. The study showed that Si can promote the enrichment of Cr and Mo and form protective oxide coating.

In this work, according to the characteristics of 625 alloy and the unique oxidation resistance of Si, the effect of Si content (0wt%, 1wt%, 3wt%, referred to as 0Si, 1Si, 3Si respectively) on the high temperature oxidation performance of laser cladding layer generated from 625 powder was investigated. According to Gibbs free energy, the morphology and phase of oxidation products were analyzed, and the effects of Si content and temperature on the oxidation mechanism were investigated. The chemical composition of the powder is shown in Table 1. In order to systematically study its mechanism, three temperature gradients of 700, 800 and 900 °C were set.

1 Experiment

1.1 Materials and laser cladding process

Rel-c3300w continuous fiber laser from Key Laboratory of Power Station Energy Transfer, Transformation and System, Ministry of Education, North China Electric Power University was used in this experiment. The laser is produced by Hubei Rui Ke Fiber Laser Technology Co., Ltd. Laser cladding system mainly includes 3.3 kW adjustable power laser, water cooling system, powder feeding system, cladding control plate, gas protection system and dust removal system, etc. The 625 metal powder used in this experiment was produced by Bei Kuang New Material Technology Co., Ltd. The oxidation characteristics of Ni-base alloy cladding layer at high temperature were studied by adding a small amount of Si in 625 alloy powder at different temperatures. The sample was prepared according to the parameters explored. The thickness of single layer was about 700 μm, and 2.5 mm high temperature oxidized sample should be guaranteed. In order to

facilitate cutting, the thickness of cladding layer should be more than six layers. After each layer was finished, it was cooled and the impurities on the surface were polished before proceeding to the next layer. The prepared cladding layer was cut by wire cutting, and the sample size was 20 mm×10 mm×2.8 mm.

1.2 High temperature oxidation

Three temperature gradients were set up in this experiment. Therefore, three samples of 625 alloy cladding layer with different silicon contents were prepared. The surfaces of these samples were wet-ground by continuous silicon carbide sandpaper from 400# to 1200#, and then cleaned and dried in ultrasonic alcohol bath for high-temperature oxidation experiment. The high-temperature oxidation instrument used in this experiment was the SX2-2.5-10N box-type resistance furnace from Shanghai Jingqi Instrument Co., Ltd. The main technical parameters are shown in Table 2.

Referring to HB 5258-2000, this experiment adopted the cyclic oxidation[16] method. Before the experiment, the sample was put into the crucible for initial mass measurement, and then the alloy cladding sample was tested with alternating hot and cold during the test, and the oxide skin was left to fall off naturally. The oxidation mass gain of the alloy cladding sample was measured after each cycle[17]. The temperature of high-temperature box-type resistance furnace was set to 700, 800 and 900 °C, and the temperature control accuracy was ±2 °C. A group of samples (0Si, 1Si, 3Si) were put at each temperature, and the samples were taken out and weighed every 24 h, which was called a cycle. After 6 cycles, the total oxidation time was 144 h. When it was heated to the preset temperature and remain stable, the measured sample was put into the high-temperature box-type resistance furnace for oxidation test. In order to ensure the reproducibility of the experiment and data consistency, each crucible holding the sample was put in a fixed position. Samples were taken according to the set experimental period, cooled to room temperature, and weighed on an electronic balance (accuracy: ±0.01 mg). Record the change of mass gain of the sample during each weighing, keep the data, put it back into the furnace, record the time, and prepare the experiment for the next cycle.

1.3 Characterization method

X-ray diffractometer (Rigaku D/Max-2400, Tokyo, Japan), scanning electron microscope (SEM, ZEISS EVO 18, Berlin,

Table 1   Chemical compositions of powders (wt%)

Sample	Si	Cr	Mo	Fe	Ni
0Si	0.5	20~23	8~10	≤5	Bal.
1Si	1.5	20~23	8~10	≤5	Bal.
3Si	3.5	20~23	8~10	≤5	Bal.

Table 2   Main technical parameters of SX2-2.5-10N box-type resistance furnace

Parameter	Value
Temperature control range/°C	100~1000
Power/ kW	2.5
Job dimension/mm	80×120×200
Voltage/V	220
Frequency/Hz	50
Average heating speed/°C·min^{-1}	>10

Germany and SEM, S-4800 HITACHI) and energy dispersive X-ray spectrometer (EDS, Bruker, Billerica, MA, USA) were used to analyze the surface morphology, element distribution and phase composition of the oxide films on the surface of 625 alloy laser cladded with different contents of Si after high temperature oxidation. The thickness of the oxide film on the cross-section after oxidation and the elements and products of the oxidation products at different positions were analyzed.

2 Results

2.1 Oxidation mass gain curve

According to HB5258-2000, the oxidation mass gain curve of the sample is drawn, the horizontal axis is time H, the vertical axis is mass gain W, and the calculation formula of oxidation mass gain per unit area is as follows:

$$W = \frac{m_2 - m_1}{S} \tag{1}$$

where m_2 is the sum mass of the sample and the crucible before the test (mg); m_1 is the sum mass of the sample and the crucible after the test (mg); S is the average surface area of the sample (cm^2).

The formula for calculating the average oxidation velocity K is:

$$K = \frac{G}{t} \tag{2}$$

where G is the oxidation mass gain per unit area (g·m^{-2}); t is the oxidation time (h).

The nonlinear fitting of oxidation mass gain curve is carried out, and the mathematical model formula is as follows[18]:

$$W = at^b \tag{3}$$

where W is the oxidation mass gain per unit area (mg·cm^{-2}); a and b are constants. The fitted equations and corresponding parameters of different samples at different temperatures are different, as shown in Fig.1.

Fig. 1 shows the oxidation kinetics curves at 700, 800 and 900 °C. It can be seen that the oxidation kinetics follows a parabolic law[16,17,19]. The fitted curve clearly shows the trend of oxidation mass gain per unit area. It can be seen that the final oxidation mass gain of samples with the same silicon content increases with the increase of oxidation temperature. The mass growth of the sample at 900 °C is significantly higher and faster than at 700 and 800 °C, which is caused by the faster diffusion of metal and air at higher temperatures. At the initial stage of oxidation, the oxidation mass basically increases linearly, and oxygen can react with elements on the surface of the sample. With the passage of oxidation time, the oxidation film forms, thus inhibiting the diffusion of oxygen in the matrix, and the oxidation rate of the interface gradually decreases, then entering into a stable mass gain. At this time, the mutual diffusion[18] has a great influence on the oxidation rate in the oxidation process.

At the same temperature, the oxidation resistance of alloy cladded with different Si contents is also different. With the increase of Si content, the oxidation kinetics curves show an ever gentler trend, indicating that the addition of Si reduces the oxidation rate of 625 alloy cladding layer. The oxidation kinetics curve of 3Si is more stable than that of 1Si.

Table 3 shows the average oxidation rate of each sample in the high-temperature oxidation test. The oxidation rates of 1Si and 3Si alloy claddings are about one order of magnitude lower than that of 0Si alloy claddings. In particular, due to the high temperature at 900 °C, the oxide film on the surface of the samples has different degrees of peeling off. Among them, the oxide film of the 0Si sample shows a large area of peeling off in powder form, and the peeling mass is greater than 1 g. The spalling degree of 1Si oxide film is relatively light. The 3Si oxide film has the least peeling off degree and is relatively compact. Its macroscopic morphology is shown in Fig. 2. According to HB 5288-83 "Method for Determination of Oxidation Resistance of Steel and Alloys", the three alloy claddings belong to complete oxidation resistance level at 700 and 800 °C. 1Si and 3Si belong to complete antioxidant level at 900 °C. 0Si belongs to the antioxidant class at 900 °C.

2.2 X-ray diffraction analysis

Fig. 3 shows the XRD patterns of the alloy cladding layer after 144 h oxidation in air. Since the oxidation products of the alloy at 700 and 800 °C are similar, only the oxidation products at 700 and 900 °C are analyzed. Considering that X-ray can penetrate the oxide film on the surface and that the oxide film may not completely cover the matrix, the equivalent peaks of The Ni-Cr-Mo phase and Ni-Mo-Si appear. As shown in the Fig. 3, when the temperature is 700 ℃, more Ni oxides are generated, and the peak value of Cr_2O_3 on the surface is small, while almost no Cr_2O_3 is
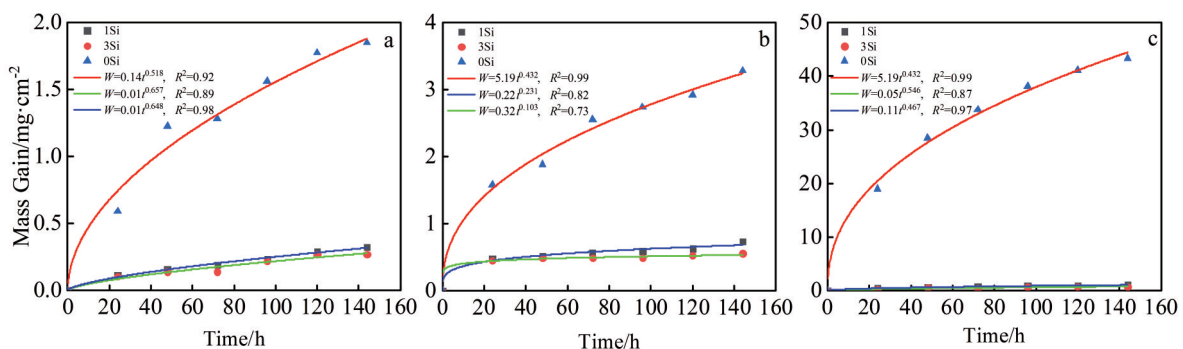
Fig.1 Oxidation kinetics curves at 700 °C (a), 800 °C (b), and 900 °C (c)

Table 3   Average oxidation rate *K* of 625 alloy cladded with different Si contents at different temperatures (g·m⁻²·h⁻¹)

Sample	700 °C	800 °C	900 °C
0Si	1.24×10^{-3}	2.28×10^{-3}	3.0×10^{-2}
1Si	2.24×10^{-4}	5.13×10^{-4}	7.73×10^{-4}
3Si	1.88×10^{-4}	3.89×10^{-4}	5.37×10^{-4}
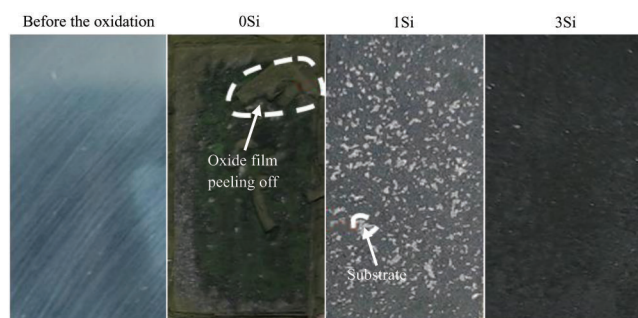
Fig.2   Macromorphologies of cladding samples with different Si contents

detected on the surface of 0Si, which is also the reason why the oxidation mass gain of 0Si alloy cladding sample is large. The Mo phase is found in 1Si and 3Si alloys, and Mo element may diffuse outwards from the matrix to form Mo oxide. In the position with small peak value, it is SiO_2. Combining the morphology of cross section oxidation products with EDS analysis, it can be determined that SiO_2 mainly exists at the junction of oxide film and matrix, thus forming an inner oxide film.

At 900 °C, due to the increase of temperature, the diffusion of oxygen and alloying elements is accelerated, and a large number of Cr and Ni oxides and their composite oxides appear, showing a more complex oxidation. In addition, it can be seen that the peak values of Cr_2O_3 and $NiCr_2O_4$ detected in 1Si and 3Si samples are higher, especially for 3Si, which generates more Cr_2O_3. It can be seen that in a certain range, with the increase of temperature and the increase of Si content, the peak value of Cr_2O_3 is improved. With the doping of Si, NiO gradually decreases, mainly manifested in the

combination of Cr_2O_3 to generate composite oxide, and with the formation of oxide film the diffusion of Ni element is prevented from the matrix.

2.3 Surface morphology and elemental analysis of oxide film

Fig.4 shows the oxidation morphologies of alloy cladding layer at 700 °C after 144 h oxidation in air. The surface is covered with massive micron oxide particles and stacked into layers. The outer layer is mainly dark gray phase, and the inner layer is light gray phase. The average size of oxide particles is in the order of 0Si>1Si>3Si. For example, at 700 °C, the diameter of 0Si, 1Si, and 3Si particles is about 50, 10, and 5 μm, respectively. The smaller the oxide particles, the denser and the more continuous the oxide film formed. It can be seen from the average oxidation rate that 700 °C belongs to the level of complete oxidation resistance, so only the phenomenon of stratification occurs but there is no serious phenomenon of oxide film shedding. As shown in Fig.4. For each alloy cladding sample, two points were selected for EDS analysis at the corresponding temperature. It can be seen that the surface of the 0Si alloy cladding sample is mainly composed of O and Ni elements, and the content of Cr element is less, and the oxides generated on the surface are mainly Ni oxides. XRD analysis shows that the surface is mainly NiO. The formation of Cr oxides is less, while NiO plays a part in the diffusion of oxygen, but its oxidation resistance is weak. When 1wt% Si is added, the outer layer shows a large amount of Cr element and a small amount of Ni element. At this time, more Cr_2O_3 has been generated, while the inner layer is dominated by Ni and Cr elements, which should be NiO, Cr_2O_3 and their composite oxides, such as $NiCr_2O_4$. When 3wt% Si is added, the composition of elements at A3 and B3 is similar, and Mo element is found in EDS spectrum of 3Si, indicating that the addition of Si promotes the diffusion of Mo element.

Fig.5 shows the surface morphologies of the alloy cladding layer after 144 h oxidation at 900 °C. At this time, due to the high temperature, the oxide film of the 0Si sample peels off seriously, and the internal oxides are exposed on the surface. The oxide particles on the surface of the alloy are loose, which cannot effectively prevent the entry of O. After Si is added, the inner oxide layer of SiO_2 can improve the binding force
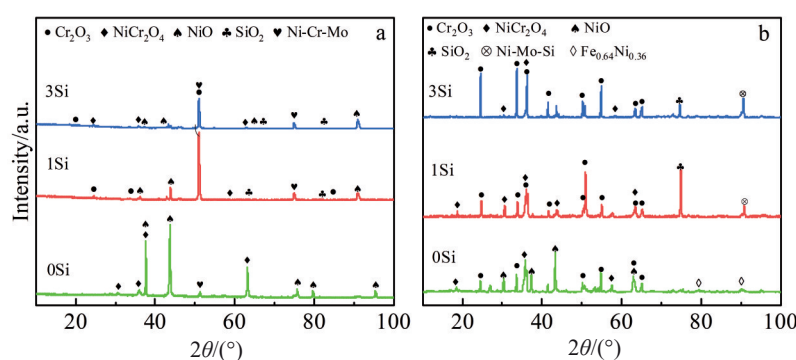
Fig.3   XRD patterns of oxidation products at 700 °C (a) and 900 °C (b)
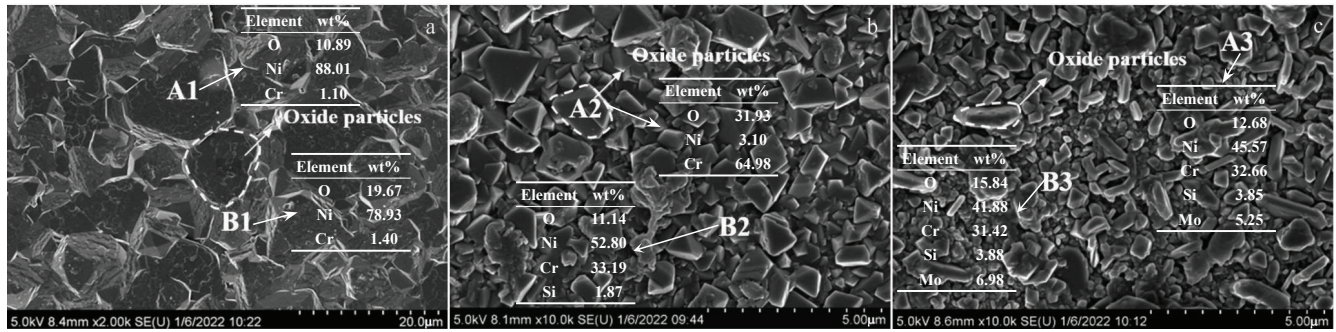
Fig.4　Oxidized surfaces of 625 alloy laser cladding layer after oxidization at 700 °C for 144 h in the secondary electron mode and EDS results of selected points: (a) 0Si, (b) 1Si, and (c) 3Si

between the oxide film and the matrix, and the spalling degree can be effectively improved. According to EDS, the content of Ni in the outer layer of 0Si and 1Si samples is higher than that of Cr, while the content of Cr in the inner layer is relatively high, indicating that the outer layer is mainly composed of oxides or composite oxides formed by nickel and nickel-chromium, while the inner layer is mainly composed of oxides of Cr. The EDS spectrum of 3Si alloy cladding layer shows that most of the surface elements are Cr and O. It can be seen that a large amount of Cr_2O_3 are generated in 3Si alloy cladding sample, and the content of Ni is very small, so the content of NiO generated is small, which is consistent with the results of XRD analysis. In addition, Mo element is also found. According to XRD, Mo element diffuses outward from the matrix to form Ni-Mo phase, and part of Mo is oxidized into MoO_2. Fe element is detected on the surface of 0Si alloy cladding sample, which diffuses outward from the matrix. It can be seen from XRD patterns that Fe-Ni phase may form, and some iron may also form complex oxides with Ni, Cr.

2.4　Cross-sectional morphology after high temperature oxidation

Fig.6 shows the cross section morphology after oxidation at 700 °C for 144 h. Table 5 shows EDS analysis of corresponding points marked in Fig. 6. Fig. 7, Fig. 8 and Fig. 9 are EDS mappings of corresponding cross-sections of Fig. 6a, 6b and 6c, respectively. It can be seen from the element mapping and section morphology that O anions are diffused internally

in different degrees and depths. The thickness of the oxide film is determined from the distribution of O element. After oxidation, O ions of 0Si 625 alloy cladding sample diffuse deeply inward, up to 1200 μm, as shown in the dark gray area (light gray area is the unoxidized matrix part). The region caused by the internal oxidation becomes the oxidation affected region, which reflects the oxidation degree of the matrix in the alloy. There are two strip inner oxidation parts in the alloy cladding matrix with Si content of 1wt%. The alloy cladded with 3wt% Si has no obvious inner oxidation phenomenon[20].

The oxide film thickness of 1Si and 3Si 625 alloy cladding samples is 200~300 μm. It can be seen that the oxide film on the surface of 1Si has a small amount of peeling off, while the oxide film on the surface of 3Si has a relatively small amount of peeling off, basically forming a continuous and dense oxide film. The growth of the oxide scale is mainly based on the outward diffusion of cations, such as Cr^{3+}, Ni^{2+}, Fe^{3+}. It can be seen from the surface sweep diagram and EDS element analysis that the oxide film is mainly composed of O, Cr and Ni, and there is a small amount of Mo element in the outer area of the oxide film, which may be a small amount of Mo oxides volatilized and covered on the surface of the oxide film. At the junction of oxide film and matrix, Si element content is high, and it can be known from the experiments of Wang[6], Du[16] et al that it is mainly SiO_2. The content of Ni in 3Si oxide film is small, and the composition of the oxide film
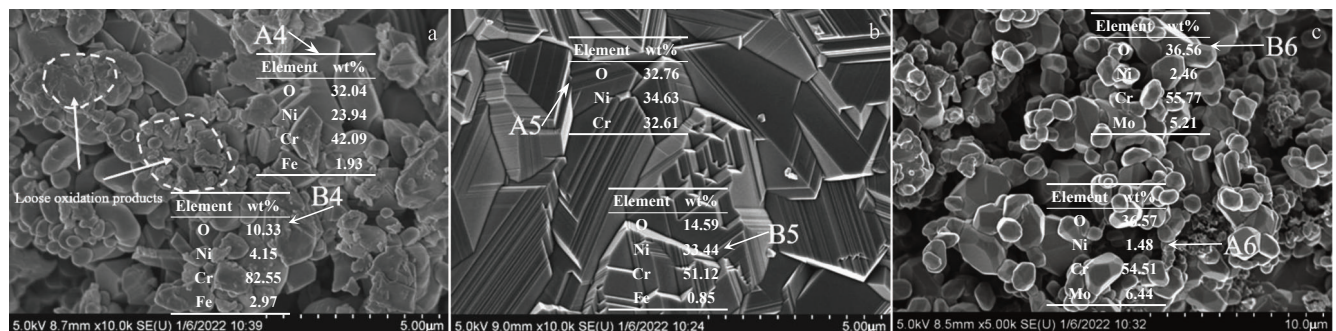
Fig.5　Oxidized surfaces of the 625 alloy laser cladding layer after oxidization at 900 °C for 144 h in the secondary electron mode and EDS results of selected points: (a) 0Si, (b) 1Si, and (c) 3Si
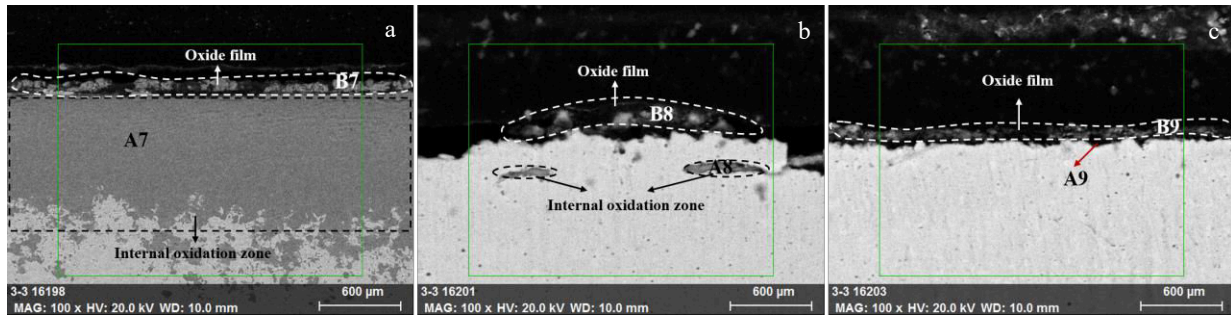
Fig.6　Cross-sectional morphologies after oxidation at 700 °C for 144 h: (a) 0Si, (b) 1Si, and (c) 3Si

Table 5　EDS analysis of the cross section of 625 alloy laser cladding layer oxidized at 700 °C for 144 h (wt%)

Alloy	Point marked in Fig.6	O	Ni	Cr	Mo	Si	Fe
0Si	A7	19.05	23.83	46.23	10.56	-	-
	B7	10.44	71.19	11.40	5.22	0.36	0.19
1Si	A8	10.82	14.78	39.88	11.27	1.47	-
	B8	13.91	36.20	42.99	4.29	2.61	-
3Si	A9	36.84	10.25	38.02	1.49	13.41	-
	B9	10.37	23.18	42.21	18.40	5.37	-
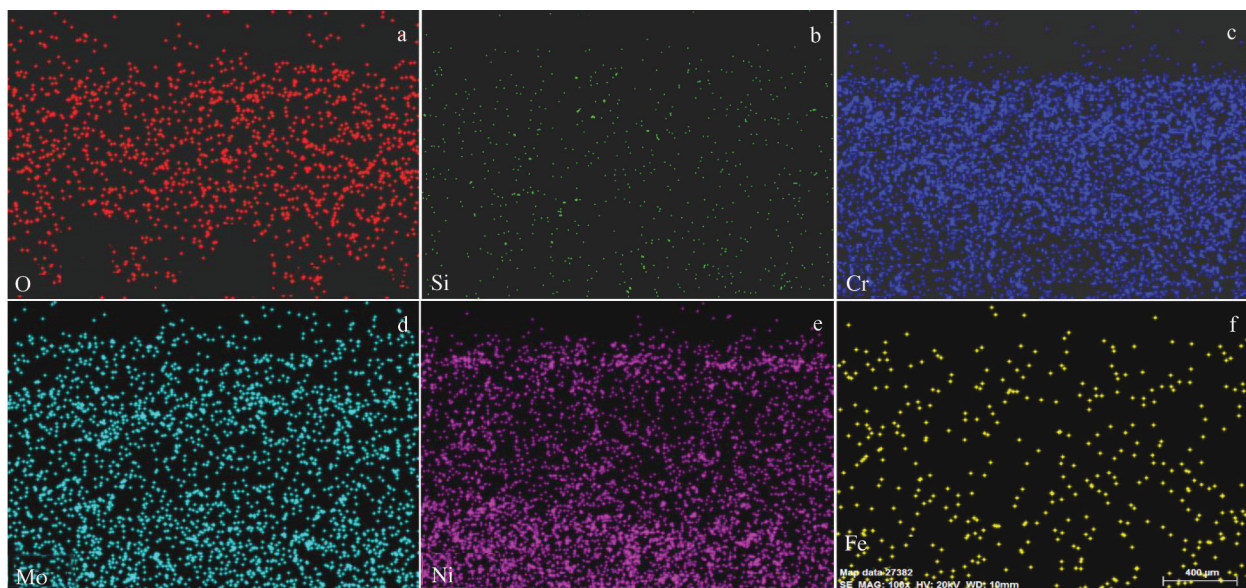
Fig.7　EDS mappings of 0Si alloy after oxidation at 700 °C for 144 h

is mainly Cr oxide and a small amount of Mo oxide, which is consistent with the XRD results. From the distribution of Fe and EDS spectrum, it can be found that the addition of Si inhibits the outward diffusion of Fe to a certain extent[7].

3　Discussion

According to the oxidation principle of the alloy, the occurrence of oxidation reaction requires that the Gibbs free energy must be less than 0, and the smaller the Gibbs free energy, the more stable the oxide. As shown in Table 6[18], the standard Gibbs free energy of oxides formed by Cr, Si, Mo and O in 625 alloy is lower than that of oxides formed by Ni

and O. Therefore, chromium oxides or molybdenum oxides should be formed first theoretically. However, the Ni content in the alloy is high, so NiO is preferentially formed at 700 °C. Ni diffuses faster than O in the formed NiO film, and NiO combines with oxygen to form new NiO. As Ni diffuses outward from the matrix through the NiO oxide film, Cr and Mo elements are enriched in 625 alloy samples, resulting in the formation of oxides such as Cr_2O_3 and MoO_2. Among them, The Gibbs free energy formed by NiO is the largest, and NiO can conduct solid phase reaction with Cr_2O_3 with abundant surface:

$$NiO + Cr_2O_3 \rightarrow NiCr_2O_4 \tag{4}$$
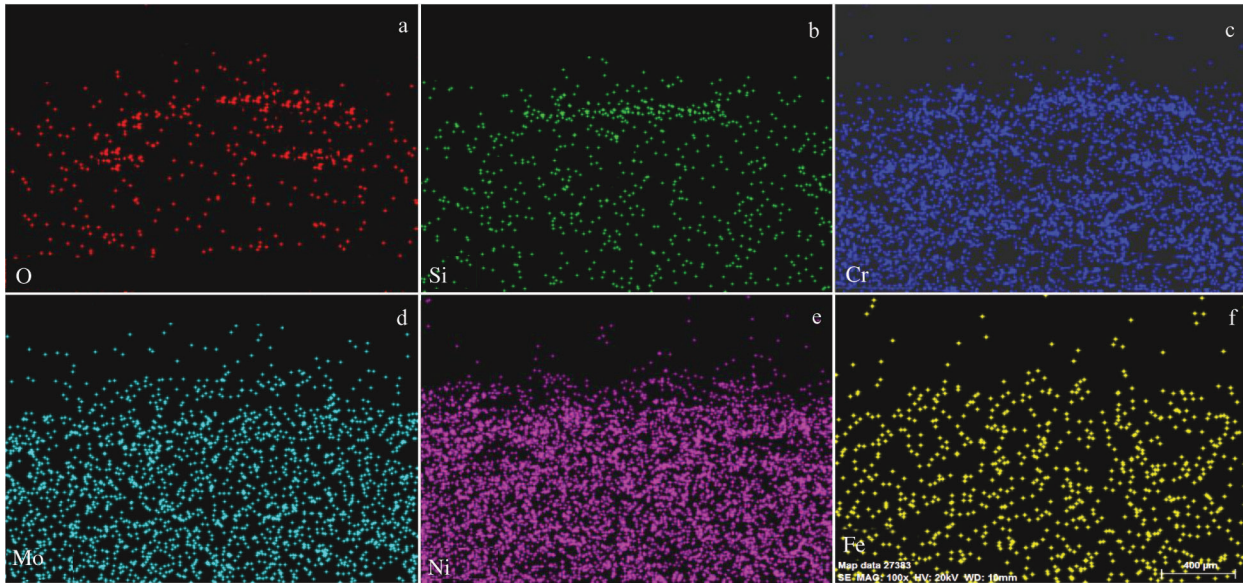
Fig.8   EDS mappings of 1Si alloy after oxidation at 700 °C for 144 h
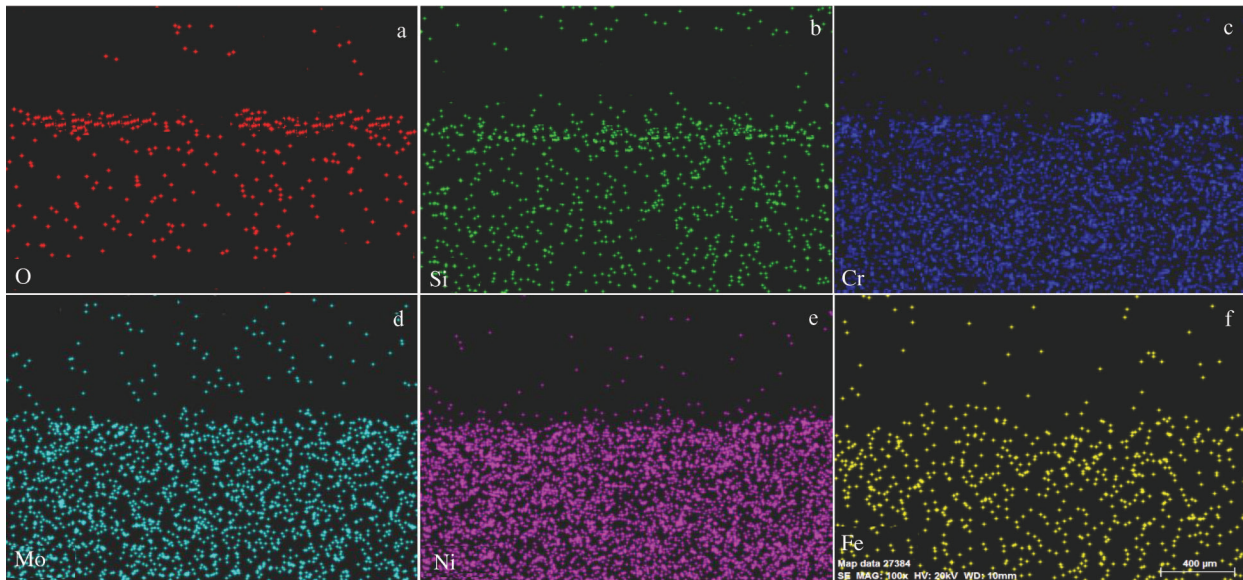
Fig.9   EDS mappings of 3Si alloy after oxidation at 700 °C for 144 h

Table 6   Standard Gibbs free energy of oxides at different temperatures (kJ·mol⁻¹)[18]

Oxide	700 °C	800 °C	900 °C
Cr_2O_3	−1263.1	−1286.7	−1310.3
NiO	−302.6	−313.4	−324.2
$NiCr_2O_4$	−1577.9	−1613.0	−1648.1

$$\Delta G^{\theta}=\Delta G^{\theta}(NiCr_2O_4)-\Delta G^{\theta}(NiO)-G^{\theta}(Cr_2O_3) \qquad (5)$$

As can be seen from the cross section scanning figure after oxidation, Ni produces a high concentration gradient between the matrix and the surface, which promotes the diffusion of Ni to form $NiCr_2O_4$. The Gibbs formation free energy of $NiCr_2O_4$ is low, so the performance is relatively stable, especially at 900 °C, and XRD shows that there are more $NiCr_2O_4$.

At the initial stage of oxidation, the surface of the alloy cladding layer is bright, as shown in Fig.2, and the oxidation products are less and the oxidation film does not completely cover the surface of the alloy. At this time, the oxidation kinetics curve shows a high oxidation rate and rapid mass gain, which is called the "interface reaction stage". The interfacial reaction rate is the main controlling factor of oxide film growth. This corresponds to the beginning of the oxidation kinetics curve. As the reaction proceeds, Cr_2O_3, SiO_2 and other oxide films are gradually generated to prevent the diffusion of oxygen elements; the interface oxidation rate gradually decreases, and the oxidation products show steady mass gain, which is the "diffusion reaction stage". At this time, the diffusion rate of oxidation atmosphere and alloying elements in the reaction plays a leading role in the growth of

oxide film, instead of the interface reaction rate. At 700 and 800 °C, this law is more obvious. At 900 °C, due to the high temperature, the oxide film will peel off to different degrees at this time, so the interfacial reaction stage takes a long time. The increase of temperature simultaneously promotes the diffusion of oxygen and alloying elements[18,21,22], resulting in the increase of oxidation products. Therefore, the oxidation rate is higher in the diffusion reaction stage.

According to the oxidation kinetics curve and oxidation rate data, the addition of Si effectively reduces the oxidation reaction rate of 625 alloy cladding sample. Si element after oxidation can generate the inner SiO_2 oxide film, and the solubility of elements such as Ni, Cr, Mo in SiO_2 is very small, so it is difficult to spread through the SiO_2 oxide layer, so as to prevent the external diffusion of matrix elements. SiO_2 also blocks the internal penetration of O anion [20], so the oxidation resistance of alloy plays a role. In addition, Si also has a certain influence on the formation of Cr_2O_3. The study shows that the addition of Si makes the Cr element on the surface of the matrix be oxidized. From the surface morphology, it can be seen that the addition of Si makes the Cr_2O_3 particles become smaller and smaller, which promotes the formation of a complete Cr_2O_3 protective film on the surface. Interestingly, on the one hand, Si can promote Cr element to form a dense oxide layer on the surface; on the other hand, continuous and dense SiO_2 grows vertically and accumulates at the interface to prevent Cr element in the inner layer of the matrix from entering the oxide film. Therefore, the combination of continuous and dense Cr_2O_3 oxide film on the surface and SiO_2 film on the inner layer is the key to the excellent oxidation resistance of the alloy cladding layer.

Among the three kinds of alloy samples cladded with different Si contents, the 0Si alloy cladding sample has obvious in-matrix oxidation phenomenon, while the 1Si alloy cladding sample has only two oxidized regions in the alloy, which are strip-like. According to EDS and EDS mapping, this region is mainly Cr oxide, and the content of Ni is less. 3Si alloy cladding sample is continuously dense due to the formation of Cr_2O_3 surface oxidation film, and the inner layer of SiO_2 oxide film hinders the internal penetration of oxygen, so there is no obvious internal oxidation phenomenon, which also reflects the rule of oxidation kinetics curve from the side.

4 Conclusions

1) The oxidation kinetics curves of the 625 alloy cladding sample with Si content ranging from 0wt% to 3wt% at 700, 800 and 900 °C all conform to the parabolic law. The 625 alloy cladded with three different contents of Si at 700, 800 °C and 1Si and 3Si at 900 °C all belong to the complete oxidation resistance level, and the 0Si alloy cladding sample at 900 °C belongs to the oxidation resistance level. In addition, the oxidation rate of 0Si alloy cladding sample is one order of magnitude higher than that of 1Si and 3Si. With the increase of Si content, the anti-spalling property of the cladding sample is improved.

2) Both 625 alloy cladding sample forms oxidation film

under high temperature oxidation, and 1Si and 3Si alloy cladding sample generate relatively dense SiO_2 inner oxidation film, and the existence of Si also promotes the formation of continuously dense Cr_2O_3 surface oxidation film. In particular, the dense SiO_2 and Cr_2O_3 in the inner layer of 3Si alloy improve the oxidation resistance.

3) Si doping can promote the diffusion of Mo element to a certain extent. The formation of oxidation film can effectively inhibit the diffusion of Fe, thus inhibiting the formation of Fe oxides, and the improvement of oxidation resistance plays a certain role.

4) The addition of Si can effectively reduce the diffusion rate of metal elements in the matrix through SiO_2 and Cr_2O_3 oxide layer and the infiltration of O element, which avoid the occurrence of large area of internal oxidation and improve the oxidation resistance of 625 alloy cladding.

References

1　Xiao Jiuhan, Xiong Ying, Wang Li *et al. International Journal of Minerals, Metallurgy and Materials*[J], 2021, 28(12): 1957

2　Mallikarjuna H T, Caley W F, Richards N L. *Journal of Materials Engineering and Performance*[J], 2017, 26(10): 4838

3　Texier Damien, Copin Etienne, Flores Agustin *et al. Surface and Coatings Technology*[J], 2020, 398: 126 041

4　Ackermann H, Teneva-Kosseva G., Lucka K *et al. Corrosion Engineering, Science and Technology*[J], 2013, 45(6): 468

5　Liu Congcong, Liu Zongde, Gao Yuan *et al. Applied Surface Science*[J], 2022, 578: 152 061

6　Wang Erpeng, Sun DuanJun, Liu Haifei *et al. Oxidation of Metals*[J], 2019, 92(3-4): 151

7　Xu Zhiyuan, Liu Shaojun, Song Liangliang *et al. Fusion Engineering and Design*[J], 2021, 167: 112 384

8　Horita Teruhisa, Kishimoto Haruo, Yamaji Katsuhiko *et al. Journal of Power Sources*[J], 2006, 157(2): 681

9　Horita Teruhisa, Yamaji Katsuhiko, Yokokawa Harumi *et al. International Journal of Hydrogen Energy*[J], 2008, 33(21): 6308

10　Jing Jing, He Jian, Guo Hongbo. *Journal of Materials Science & Technology*[J], 2019, 35(9): 2038

11　Yun D W, Seo S M, Jeong H W *et al. Corrosion Science*[J], 2014, 83: 176

12　Wang Qinying, Zhang Yangfei, Bai Shulin *et al. Journal of Alloys and Compounds*[J], 2013, 553: 253

13　Chang Fa, Cai Bingjie, Zhang Chong *et al. Surface & Coatings Technology*[J], 2019, 359: 132

14　Yang Yu, Wang Aihua, Xiong Dahui *et al. Surface & Coatings Technology*[J], 2020, 384: 125 316

15　Scendo M, Staszewska-Samson K, Danielewski H. *Coatings*[J], 2021, 11(7): 759

16　Du H Q, Tian S G, Yu X F *et al. Rare Metal Materials and Engineering*[J], 2008, 37(9): 1555

17　Li Dongsheng, Chen Guang, Li Dan *et al. Rare Metals*[J], 2018, 40(11): 3235

18 Saber D, Emam I S, Abdel-Karim R. *Journal of Alloys and Compounds*[J], 2017, 719: 133

19 Emam I S, Saber D, Waheed A. *Journal of Testing and Evaluation*[J], 2020, 48(2): 1277

20 Meng X X, Pei Y W, Shao W *et al. Corrosion Science*[J], 2018, 133: 112

21 Aghayar Y, Khorasanian M, Lotfi B. *Materials at High Temperatures*[J], 2018, 35(4): 343

22 Zhang Zhaoning, Kong Ning, Li Hongbo *et al. Materials Research Express*[J], 2018, 5(6): 665 06

Si对625合金激光熔覆层高温氧化特性的影响

张　剑，刘宗德，马荷蓉，李　悦，李家璇

(华北电力大学 电站能量传递转化与系统教育部重点实验室，北京 102206)

摘　要：利用循环氧化法，研究了不同Si含量（0%，1%，3%，质量分数）的625合金熔覆层在700、800、900 ℃下氧化144 h后的高温氧化行为。用XRD分析了氧化物相。通过SEM/EDS研究了氧化物表面和截面的形貌、元素组成和氧化膜的厚度。结果表明，不同温度下试样的氧化动力学都保持抛物线规律，随着温度的升高，氧化增重逐渐增加。通过观察，在900 ℃时，0% Si含量的625合金熔覆层出现了氧化膜大面积剥落的情况，3% Si含量的合金熔覆层氧化膜保持完整。在700 ℃时，随着Si含量增加，氧化膜表面的氧化颗粒尺寸减小且更加致密，同时促进了Cr_2O_3氧化物的生成。在700 ℃下，0 % Si含量的试样出现了大片的内氧化区域；1% Si含量的试样基体部分出现了2处条状的含Ni，Cr，Mo的氧化物相区；而3% Si含量的试样氧化后由于生成了富Si的内氧化层，这阻止了内氧化的发生。外层Cr_2O_3氧化膜和内层SiO_2的联合作用既阻止了O阴离子的渗入也抑制了Fe等金属离子的扩散，提高了合金熔覆层的抗氧化性。

关键词：激光熔覆；625合金；氧化动力学；氧化膜；扩散

作者简介：张　剑，男，1997年生，硕士，华北电力大学电站能量传递转化与系统教育部重点实验室，北京 102206，电话：010-61772277，E-mail：120202202118@ncepu.edu.cn